A broadband LNA and mixer for digital video broadcasting applications using a 0.18-m CMOS process

Article *in* Microwave and Optical Technology Letters · September 2015

DOI: 10.1002/mop.29267

5 authors, including:

Tian Qiang
Jiangnan University
27 PUBLICATIONS **117** CITATIONS
SEE PROFILE

Eun Seong Kim
Kwangwoon University
39 PUBLICATIONS **193** CITATIONS
SEE PROFILE

Cong Wang
Harbin Institute of Technology
151 PUBLICATIONS **1,155** CITATIONS
SEE PROFILE

Min-Chul Park
Korea Institute of Science and Technology
339 PUBLICATIONS **1,675** CITATIONS
SEE PROFILE

generates Σ and Δ patterns of two received signals. Antenna array and coupler were integrated and Σ–Δ patterns obtained, in vertical and horizontal directions, by constructing two separate same design circuits: one for finding DOA for θ_1 and other circuit finding DOA for θ_2. By putting Σ–Δ patterns in Eq. (3), AOA has been estimated. This task first has been simulated in ADS layout and optimized for expected results. Later, simulated designs of both circuits were fabricated on RT Duroid 5880 substrate. Each circuit's 3D Σ–Δ patterns were taken as measured data. Experimentally obtained data was imported in Matlab for analysis of DOA. Measured *S*-parameters and far field Σ–Δ patterns are very close to simulated results. From Σ–Δ patterns of each circuit, DOA has been estimated for both axis. Both circuits are able to find direction of received signal from 0 to ±40° in their respective axis. For performance measurement, rms error also has been calculated which is less than 5° in both circuits. However, it increases more as we go above the 40° which suggests that designed DOA system works well for 0 to ±40°. By looking at all simulated and measured results, proposed system design of DOA works in satisfactory range which in result fulfills the purpose of this article.

REFERENCES

1. A. Vesa and G. Iozsa, Direction – of – arrival estimation for uniform sensor arrays, In: 9th International Symposium on Electronics and Telecommunications, Timisoara, 2010, pp. 249–252.
2. R. Tanaka, E. Nishiyama, and I. Toyoda, A mono-pulse DOA estimation antenna integrated with RF amplifiers and detection circuits, In: IEEE Antennas and Propagation Society International Symposium (APSURSI), Memphis, TN, 2014, pp, 1833–1834.
3. H. Sakai, E. Nishiyama, and I. Toyoda, Direction of arrival estimating array antenna, In: Proceedings of International Symposium on Antennas and Propagation, Nagoya, Japan, 2012, pp. 1124–1127.
4. M. Rubsamen and A. Gershman, Direction – of – arrival for non-uniform sensor arrays: From manifold separation to Fourier domain MUSIC methods, IEEE Trans Signal Process 57 (2009), 588–599.
5. W.L. Stutzman and G.A. Thiele, Antenna theory and design, 2nd ed., Wiley, New York, 1998.
6. J.M. Rathod, Comparative study of microstrip patch antenna for wireless communication application, Int J Innov Manag Technol 1 (2010).
7. K.-L. Wong, Compact and broadband microstrip antennas, Wiley, Hoboken, NJ, 2002.
8. E. levine, G. Malamud, S. Shtrikman, and D. Treves, A study of microstrip array antennas with the feed network, IEEE Trans Antennas Propag 37 (1989), 426–434.
9. R.E. Munson, Conformal microstrip antennas and microstrip phased array, IEEE Trans Antenna Propag AP-22 (1974), 74–78.
10. J.J. Huang, A technique for an array to generate circular polarization with linearly polarized elements, IEEE Trans Antenna Propag AP-34 (1986), 1113–1124.
11. M.H. Nemati, R. Kazemi, and I. Tekin, Pattern reconfigurable patch array for 2.4 GHz WLAN systems, Microwave Opt Technol Lett 56 (2014), 2377–2381.
12. G.C. Hock and C.K. Chakrabarty, Design of a 5.8 GHz rat-race coupler on the R04003C® substrate, In: 2006 International RF and Microwave Conference Proceedings, Putra Jaya, 2006, pp. 253–257.
13. J.T. Kuo and C.H. Tsai, Generalized synthesis of rat race ring coupler and its application to circuit miniaturization, IEEE Trans Microwave Theory Tech (2008).
14. D.M. Pozar, Microwave engineering, 3rd ed., Wiley, New York, 2005.

A BROADBAND LNA AND MIXER FOR DIGITAL VIDEO BROADCASTING APPLICATIONS USING A 0.18-μM CMOS PROCESS

Tian Qiang,[1] Eun Seong Kim,[1] Cong Wang,[1] Min Chul Park,[2] and Nam Young Kim[1]
[1] RFIC Center, Kwangwoon University, 447-1 Wolgye-dong, Nowon-ku, Seoul 139-701, Korea; Corresponding author: nykim@kw.ac.kr
[2] Sensor System Research Center, Korea Institute of Science and Technology, Hwarang-ro-14-gil, Seongbuk-Gu, Seoul 139-791, Korea

Received 23 February 2015

ABSTRACT: *In this study, a broadband low noise amplifier (LNA)/mixer for digital video broadcasting-satellite receiver tuner was fabricated by a 0.18-μm complementary metal oxide semiconductor (CMOS) process. The proposed broadband LNA receives positive feedback and incorporates a single-ended differential converter to mixer. Two attenuators are used to obtain good noise performance and high linearity. Moreover, the designed CMOS LNA/mixer achieved gain controls in 3-dB steps, an input second-order intercept of 1.37 dBm, and an input third-order intercept of −3.6 dBm in high-gain low-frequency mode. The 6.4-dB noise of LNA was achieved in the frequency range of 950–2150 MHz. The circuit consumes a total current of 25 mA at a supply voltage of 1.8 V and the chip area of the LNA and the mixer are 0.8 × 0.53 mm² and 0.8 × 0.6 mm², respectively.* © 2015 Wiley Periodicals, Inc. Microwave Opt Technol Lett 57:2092–2099, 2015; View this article online at wileyonlinelibrary.com. DOI 10.1002/mop.29267

Key words: *low noise amplifier; mixer; digital video broadcasting-satellite; complementary metal oxide semiconductor; broadband*

1. INTRODUCTION

Digital video broadcasting-satellite (DVB-S2) is a digital television broadcast standard that has been designed as a successor for the popular DVB-S system [1–3], which was developed in 2003 by the DVB Project [4]. The standard is based on and improves on DVB-S and the digital satellite news gathering system, which is used by mobile units for sending sounds and images from remote locations world-wide back to their home television stations [5]. DVB-S2 achieves significantly better performance than its predecessors, allowing for an increase of available transmission capacity over the same satellite transponder bandwidth. The measured DVB-S2 performance gain over DVB-S is approximately 30% at the same satellite transponder bandwidth and emitted signal power [6]. The primary goals of standard revision are to guarantee a much higher transmission capacity and to improve service capabilities through enhanced link margins and the realization of a new service requirements for broadband broadcasting, such as HDTV, interactive services, internet access, digital TV contributions and news gathering, and so forth [7]. However, there is a bandwidth limitation of the DVB-S1 system, such as the Ka-band satellite broadcasting, and the carrier-to-noise (*C*/*N*) ratio has been estimated at approximately 0.5 dB/s during heavy rain fades for the first version of DVB-S [8,9].

Regarding DVB-S2, the low noise amplifier (LNA)/mixer is designed and fabricated using the dominant integrated-circuit manufacturing technology—complementary metal oxide semiconductor (CMOS). The main advantage of CMOS over n-metal-oxide-semiconductors (NMOS) and bipolar technology is its reduced power dissipation. Unlike NMOS or bipolar circuits, a CMOS circuit has almost no static power dissipation. Power is only dissipated if the circuit actually switches, which allows the

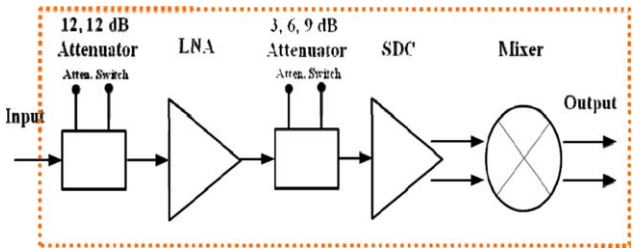

Figure 1 Block diagram of the RF front-end. [Color figure can be viewed in the online issue, which is available at wileyonlinelibrary.com]

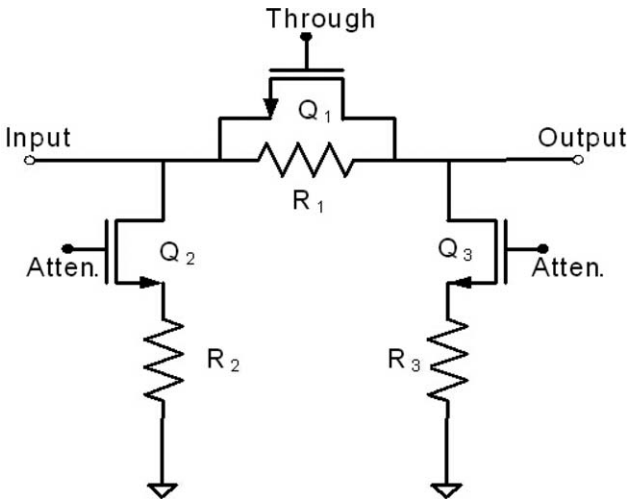

Figure 2 The designed 12-dB attenuator

integration of many more CMOS gates on an IC compared with NMOS or bipolar technology, resulting in much better performance [10]. Using this technology, the LNA/mixer achieves low-dissipation and a compact size. It can be predicted that CMOS will remain as a mainstream technology in the foreseeable future technologies, and there remains significant opportunity for further reducing the dimensions of CMOS devices. In addition, device performance will likely improve as continued efforts contribute to technology scaling over the next decade [11]. The block diagram of the proposed LNA/mixer is shown in Figure 1.

In this study, by applying positive feedback to the LNA and adding a single-ended differential converter (SDC) to the mixer, a broadband 950–2150 MHz is obtained for the application of a DVB-S2 system. In addition, a 12-dB attenuator and 3·6·9 attenuator are applied in front of and behind the LNA, respectively, to obtain a superior noise performance and high linearity.

2. CIRCUIT DESIGN TECHNIQUES

2.1. Attenuator

Attenuators are used to control the gain mode by varying the power of the input signal. To accommodate large signals and strong blockers, a gain step is necessary for the LNA to realize the linearity requirements of the mixer. The proposed attenuators are designed in pi (π) type, and the gain is controlled in 3-dB steps using 12-dB and 3·6·9 dB attenuators.

2.1.1. 12-dB Attenuator. Figure 2 shows the proposed 12-dB attenuator. By cascading two 12-dB attenuators, a total attenuation of 24 dB is obtained. The cascaded attenuators operate via two paths: the "through path" and the "attenuation path." The two paths separate the gain into three mode, which are high-gain mode, medium gain mode, and low-gain mode. When the channel of Q_1 is on and the channels of Q_2 and Q_3 are off, most signals pass through the channel of Q_1, or the "through path." In this condition, the channel resistance and parasitic capacitance of Q_1 can attenuate the signal. Therefore, the size of Q_1 is considered to be large. However, if the size of Q_1 is too large, the parasitic capacitance also increases. When the channel of Q_1 is off and the Q_2 and Q_3 channels are on, the signals pass through the pi (π) attenuator, or the "attenuation path." In addition, the channel resistances and the parasitic capacitances of Q_1, Q_2, and Q_3 affect the amount of attenuation and the frequency characteristics. In general, two cascaded 12-dB attenuators can form 12 or 24 dB attenuation modes. Figure 3 shows that the simulation and measurement results of S_{21} in 12-dB and 24-dB attenuation modes are in good agreement. The flatness of the total gain at each attenuation mode is under 3 dB.

2.1.2. 3·6·9 dB Attenuator. Figure 4 shows the presented 3·6·9 dB attenuator. The 3·6·9 dB attenuator controls the gain using 3-dB steps at each gain mode, which is separated by a 12-dB attenuator. The position of the 3·6·9 dB attenuator is next to LNA so that it does not strongly affect noise. As shown in

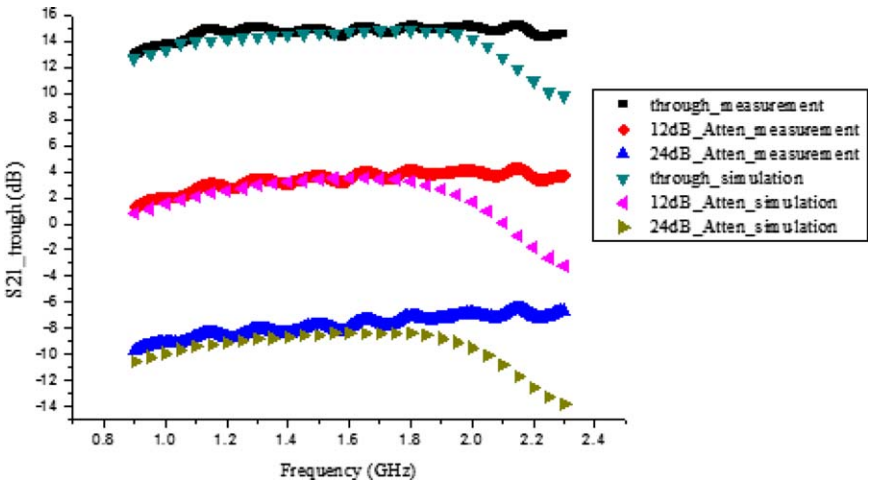

Figure 3 The simulated and measured results of S_{21} for 12-dB and 24-dB attenuation modes. [Color figure can be viewed in the online issue, which is available at wileyonlinelibrary.com]

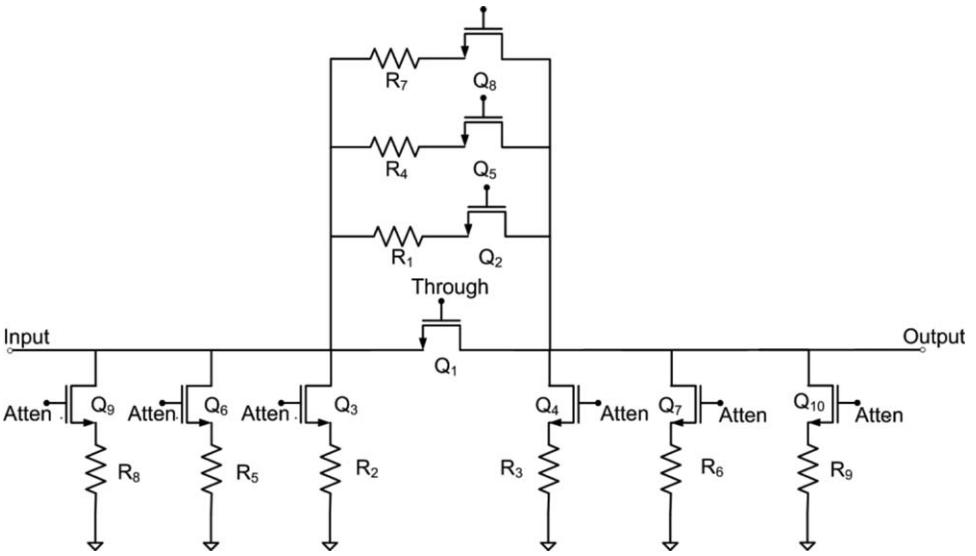

Figure 4 The designed 3·6·9 dB attenuator

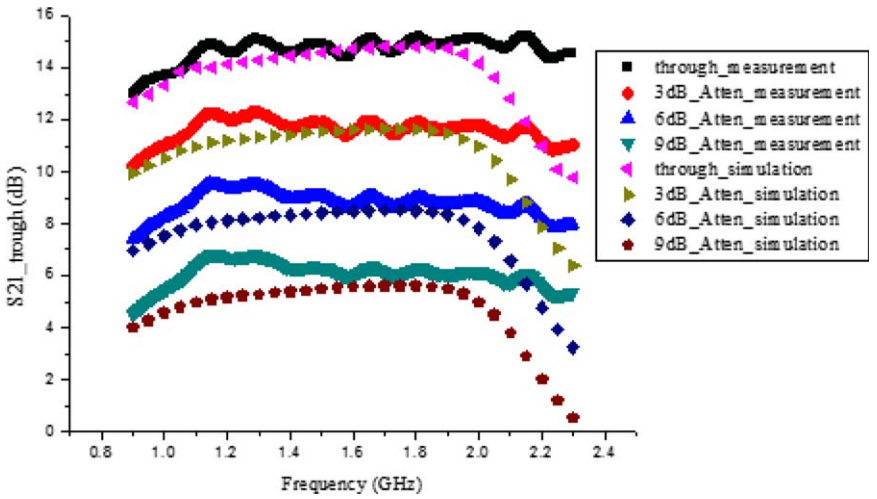

Figure 5 The simulated and measured results of S_{21} for the 3·6·9 dB attenuator modes. [Color figure can be viewed in the online issue, which is available at wileyonlinelibrary.com]

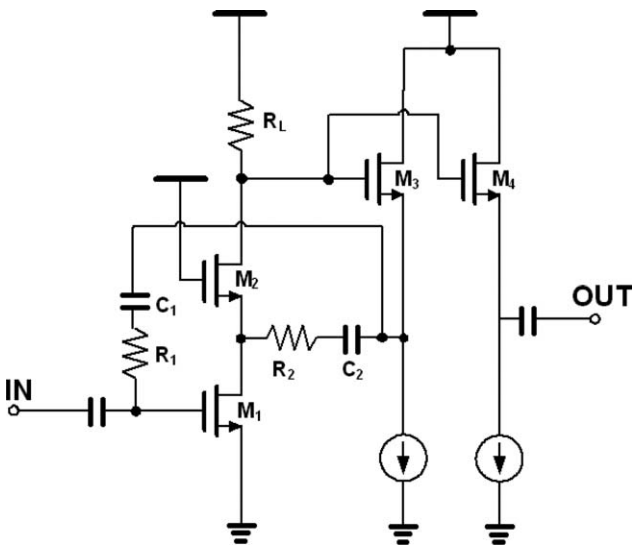

Figure 6 The inductorless LNA using positive feedback

Figure 4, each transistor and resistor of the 3-dB, 6-dB, and 9-dB attenuator is connected in parallel. When the Q_1 channel is on and the other channels are off, most signals pass through the Q_1 channel, which is termed the through mode. When the Q_1 channel is off and the Q_2, Q_3, and Q_4 channels are on, most signals pass through the pi (π) attenuator. Therefore, it can be concluded that if the channels of Q_2, Q_3, Q_4; Q_5, Q_6, Q_7; or Q_8, Q_9, Q_{10} are on, the signals pass through the 3-dB, 6-dB, or 9-dB attenuator, respectively, which are termed the 3·6·9 dB attenuation modes. The Q_1 channel is always off in attenuation mode. In general, the circuit shown in Figure 3 can form two modes: the through mode or the 3·6·9 dB attenuation modes. Figure 5 shows S_{21} for the through mode and the 3·6·9 dB attenuation modes. The attenuation quantity of the simulation and the measurements in the frequency range of from 950 to 2150 MHz is approximately 2.6–3.1 dB.

2.2. LNA

In designing the broadband LNA, the LNA must provide gain to weak signals from the antenna and the least possible contribution

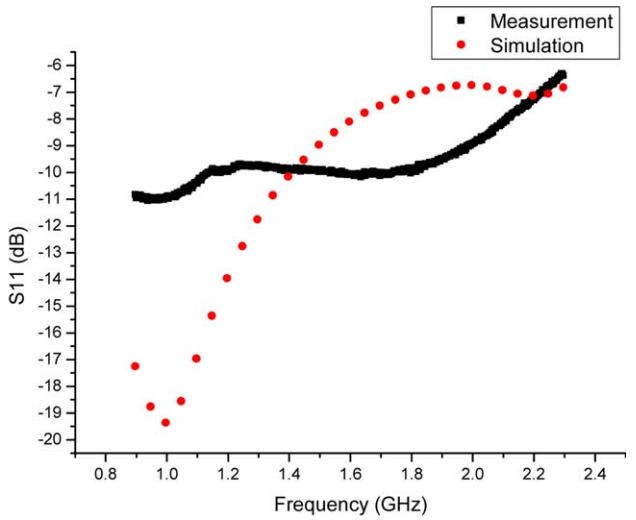

Figure 7 (a) The results of S_{11} in high-gain mode of the LNA and (b) the results of S_{21} in high-gain mode of the LNA. [Color figure can be viewed in the online issue, which is available at wileyonlinelibrary.com]

to noise so that the signal to noise ratio is not lowered by the circuit. The LNA must also be able to handle large signals without distortion. The design of a LNA involves numerous tradeoffs. The amplifier must have sufficient gain to overcome the issue of mixer noise but not too high a gain to cause mixer overload. Good noise characteristics are preferred while achieving the desired input and output matching. The matching networks at the input and output of the LNA often require a compromise between optimum gain matching and optimum noise figure matching.

The LNA occupies a significant percentage of the total die area in the wireless front-end of the DVB-S2 because the performance of the LNA is dependent on the Q-value of the on-chip inductors. The design of these circuits usually requires a larger die size and a higher number of simulation and verification iterations. Figure 6 shows an inductorless broadband LNA that uses positive feedback, which significantly reduces the cost of the wireless front-end implementation of the DVB-S2. Generally, a 75-Ω termination is used for minimum distortion characteristic in DVB-S2 receivers. Therefore, the input termination of

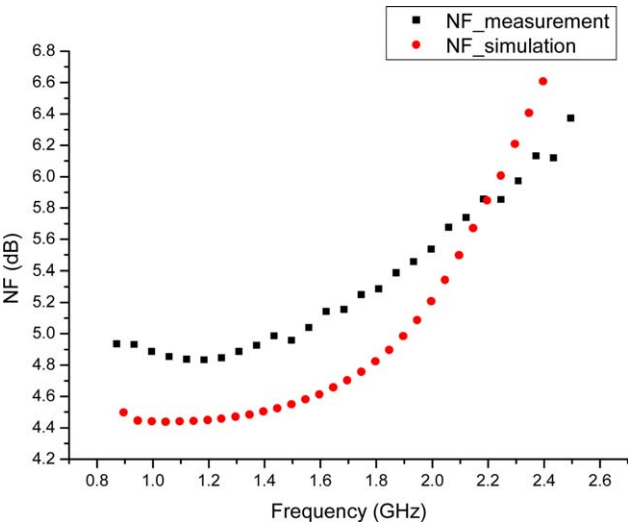

Figure 8 The results of noise in high-gain mode of the designed LNA. [Color figure can be viewed in the online issue, which is available at wileyonlinelibrary.com]

the LNA core is 75 Ω, and the output termination is 50 Ω due to the input impedance of the SDC. The LNA must feature 75-Ω input matching, good gain flatness, and a low noise figure over the entire bandwidth [12].

The common-source cascaded amplifier is the most commonly used circuit topology for LNAs, which is used to reduce the Miller effect, M_1, of the input device and to achieve improved reverse isolation due to the high output impedance, M_2, at the drain of the cascaded device. The chosen supply voltage is 2.7 V and is supplied by a low drop output (LDO). The LDO transforms the supply voltage from 3.3 to 2.7 V. The parasitic capacitance C_L and R_L create a pole and limit the bandwidth of the amplifier. A positive feedback capacitance C_2 compensates for the parasitic capacitance C_L and improves the bandwidth. The input impedance at moderate frequencies is

$$R_{in} \cong \frac{R_F}{1+A_V} \cong \frac{R_F}{A_V} \tag{1}$$

where A_V is the voltage gain. The proper choice of R_F provides input matching. However, even with the positive feedback capacitance C_2, the amplifier still has a limited bandwidth. Typically, only R_F is included, and the input matching degrades at higher frequencies due to gain roll-off and input capacitance. Matching can be enhanced with off-chip input inductance, such as a bond wire, and by properly sizing R_L, M_3, and I_3. The input impedance of M_3 is inductive, given by

$$L_{EQ} \cong C_{gs3}\frac{R_L}{g_{m3}} = \frac{R_L}{2\pi f_{t3}} \tag{2}$$

L_{EQ} can be chosen to resonate with this parasitic capacitance. A separate source follower M_4 provides better reverse isolation and the required capability to the drive SDC. The output current of M_4 is typically sent to the SDC through the 3·6·9 dB attenuator.

The simulation result of S_{11} is less than 6.8 dB, and the measurement result is below 7.7 dB in Figure 7(a). The simulation and measurement results of S_{21} in high-gain mode are shown in Figure 7(b). S_{21} is 12–14.8 dB for the simulation and 13.5–15.2 dB for the measurement. Figure 8 shows the simulation and measurement results of the noise, which is under 5.6 dB for the

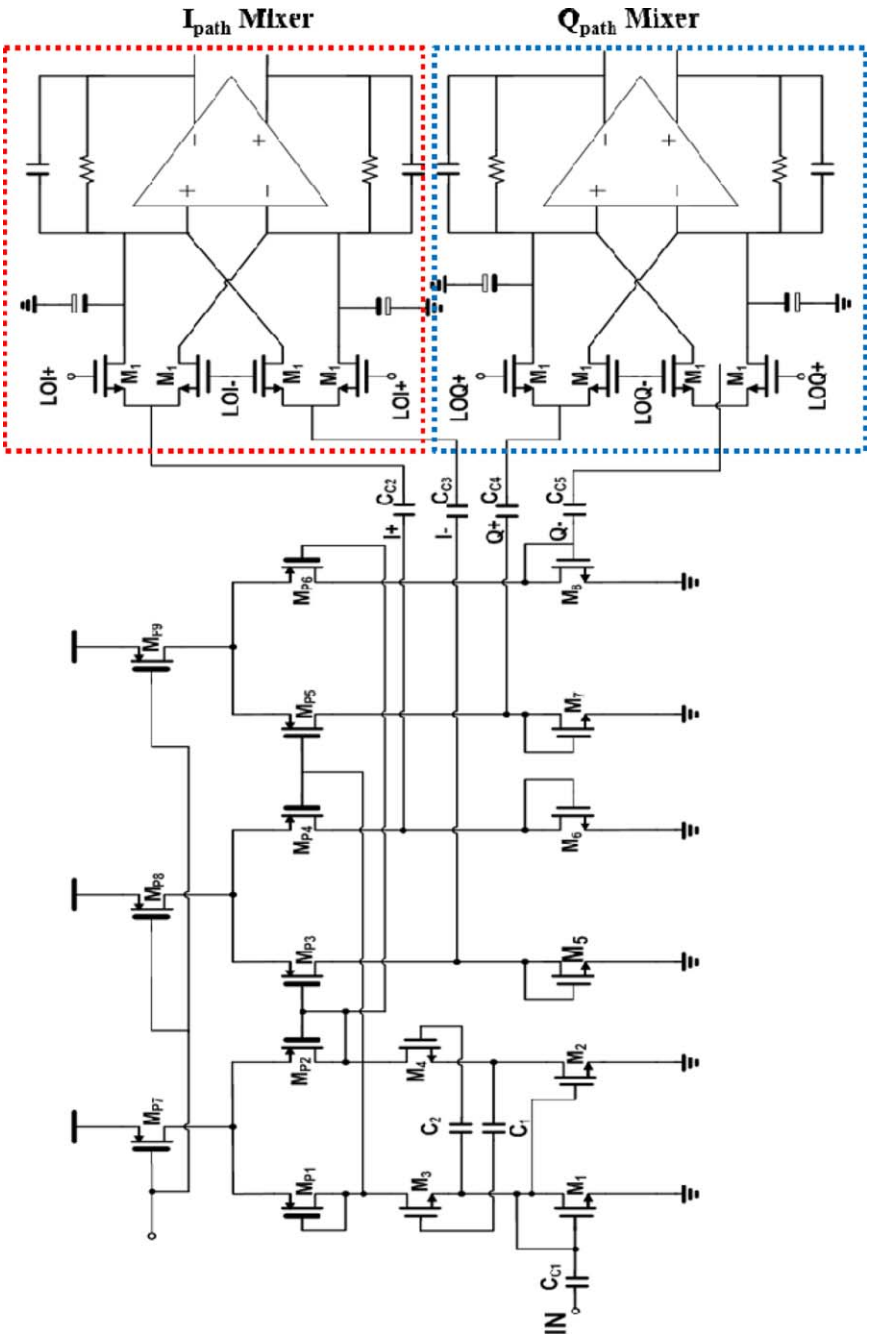

Figure 9 The designed SDC and passive mixer. [Color figure can be viewed in the online issue, which is available at wileyonlinelibrary.com]

simulation and under 5.7 dB for the measurement. The noise measurement was performed using a noise figure meter in a shielded room.

2.3. Mixer

Figure 9 shows the SDC and quadrature down-conversion mixer. The SDC converts the single output signal of the LNA to differential output signals and acts as a transconductor with an equivalent current gain (gm). By applying a current mirror structure, the SDC exhibits good broadband characteristics and high linearity to endure strong analog/digital adjacent channel interference signals. The positive channel metal oxide semiconductor (PMOS) transistors (M_{P1} and M_{P4}, M_{P5}, M_{P2}, and M_{P3}, M_{P6}) comprise a current mirror, which can amplify AC/DC current at size ratios of $(W_{P4}/L_{P4})/(W_{P1}/L_{P1})$ and $(W_{P2}/L_{P2})/(W_{P3}/L_{P3})$. However, the size ratios of this circuit are 1 and 1. If the amplified signal through the LNA is reamplified by the SDC, this front-end cannot achieve high linearity.

Each signal from the LNA is converted to differential signals by M_1 and M_2. The sizes of M_1 and M_2, M_3 and M_4 are determined by minimizing the amplitude mismatch between the differential signals. The impedances of M_1 and M_3 at node A and M_2 and M_4 at node B should be equivalent to obtain signals with equal amplitudes at the drains of M_1 and M_2, and the value is approximately 1/gm. The resistance of the diode-connected load is relatively small ($\approx$1/gm), which enables the current mirror circuit to have a flat gain response in a wideband. The current sources (M_{P7}, M_{P8}, and M_{P9}) that improve the amplitude and phase mismatch of the differential current signals are decreased by forming the two diode-connected loads into a

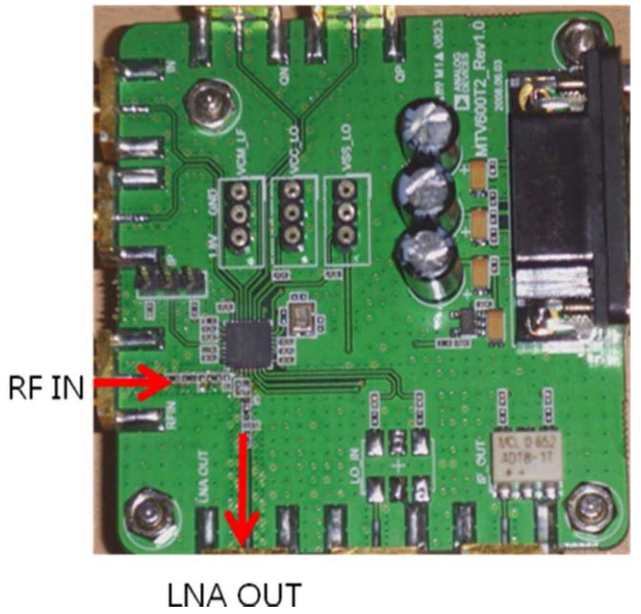

Figure 10 A photograph of the packaged chip on the PCB board. [Color figure can be viewed in the online issue, which is available at wileyonlinelibrary.com]

differential pair. However, poor linearity may result by not allowing for sufficient headroom. For this reason, the current mirror load and the current source use 3.3-V PMOS instead of 1.8-V PMOS and 2.7-V V_{DD} supplied by an external voltage regulator. To further decrease the phase mismatch, 1-pF metal-insulator-metal capacitors are used as the cross-coupling capacitors C_1 and C_2, which are added to the common gate amplifier. Two current mirror stages are added to drive the current to the quadrature passive mixer [13].

Down-conversion is performed by two (I_{path} and Q_{path}) double-balanced mixers, each consists of four MOS transistors operating in the triode region, as shown in Figure 9. The LO signals are AC-coupled to the mixers, which can improve the I-Q balance and allow for optimization of the DC bias of the switching pairs for noise and linearity. Choosing a static overdrive voltage close to zero drastically reduces the flicker noise contribution while providing excellent linearity. To achieve high linearity, low noise, and reduced LO radiation, the mixer should have a very low impedance load. However, the conversion gain is proportional to the feedback resistance. Loading the mixer with the virtual grounds of a fully differential operational amplifier with two 500-Ω resistors connected in feedback achieves both objectives. The opamp noise must be minimized for two reasons. First, the connection of both the I_{path} and Q_{path} mixers to the LNA output causes a transconductance loss of approximately 3 dB. Second, there is an equivalent resistor across the two virtual ground nodes that is produced by switching the parasitic capacitors at the LNA side that amplify the opamp noise [14]. The simulation is performed using Cadence Spectre RF. An LNA and a mixer with the SDC are simulated for DVB-S2 receiver Tuner IC applications. The total power consumption is 45.9 mW, and the current consumption is 25.5 mA, which corresponds to 19.5 mA for the LNA and 6 mA for the mixer.

3. FABRICATION AND MEASUREMENT

The broadband LNA and mixer are fabricated using Taiwan Semiconductor Manufacturing Company's 0.18-μm Mixed Mode RF 1P6M process. The fabricated multiproject wafer chips are packaged in a 5 × 5 mm^2 Quad Flat No-lead Package (QFN). A photograph of the packaged chip is shown in Figure 10.

Figure 11 shows the S_{11} and noise figure simulation results of the SDC. The S_{11} of the SDC is (1/2 gm) + α for the common gate structure, which is over 60 Ω in the frequency range of 950–2150 MHz. In addition, the noise is 12.3–13.1 dB. Figure 12 shows the phase mismatch of the SDC. The phase mismatches at 950 MHz, 1550 MHz, and 2150 MHz are 179.1°, 178.7°, and 179°, respectively. The amplitude mismatches at 950 MHz, 1550 MHz, and 2150 MHz are 1.45 μA, 10.8 μA, and 29.6 μA, respectively, or approximately 0.3–8% as shown in Figure 13. The measurement results of IIP3 and IIP2 are shown in Figure 14. IIP2 and IIP3 of the SDC are 38.1 dBm and 11.8 dBm, respectively. Finally, grounding is also very important in designing RF circuits. In this design, the LNA has four grounds, and the SDC has two grounds. The 12-dB and 3·6·9 dB attenuators have a total of three ground capacitances.

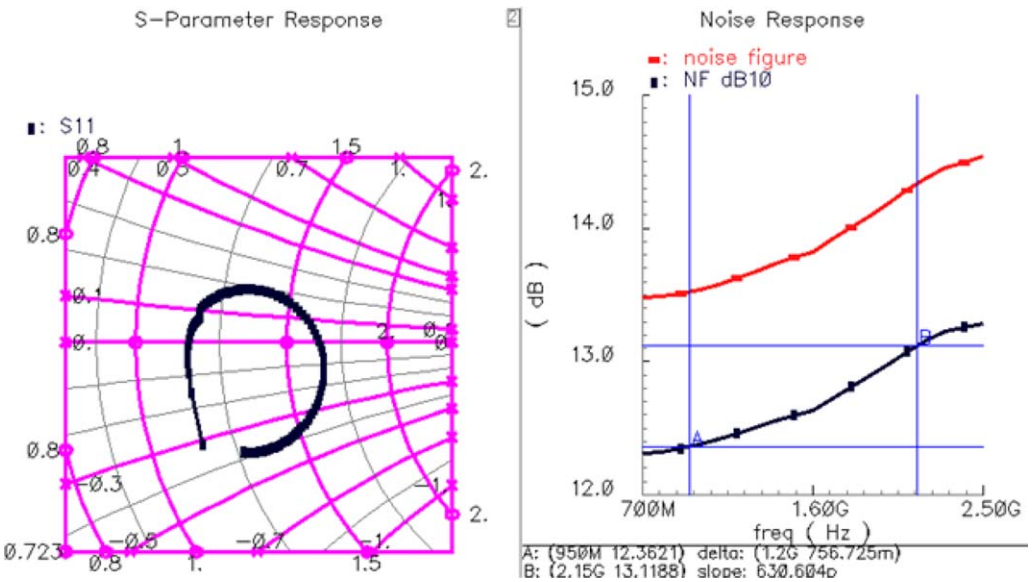

Figure 11 The measured results of S_{11} and noise. [Color figure can be viewed in the online issue, which is available at wileyonlinelibrary.com]

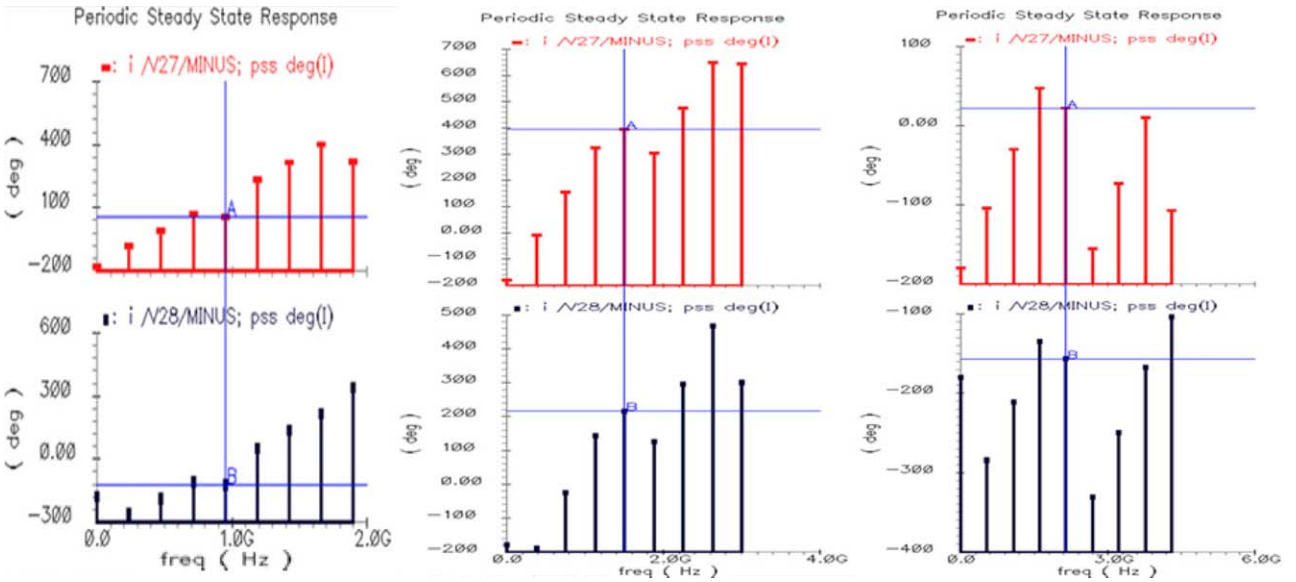

Figure 12 The measured results of the phase mismatch of the SDC. [Color figure can be viewed in the online issue, which is available at wileyonlinelibrary.com]

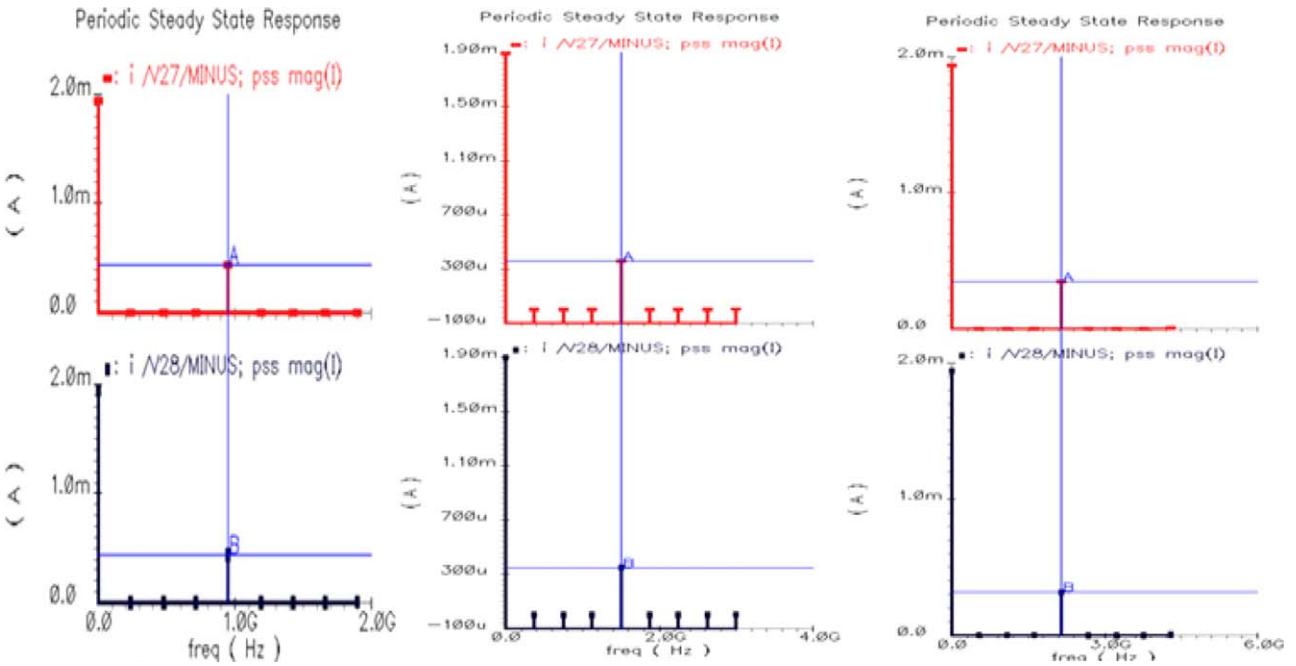

Figure 13 The measured results of the amplitude mismatch of the SDC. [Color figure can be viewed in the online issue, which is available at wileyonlinelibrary.com]

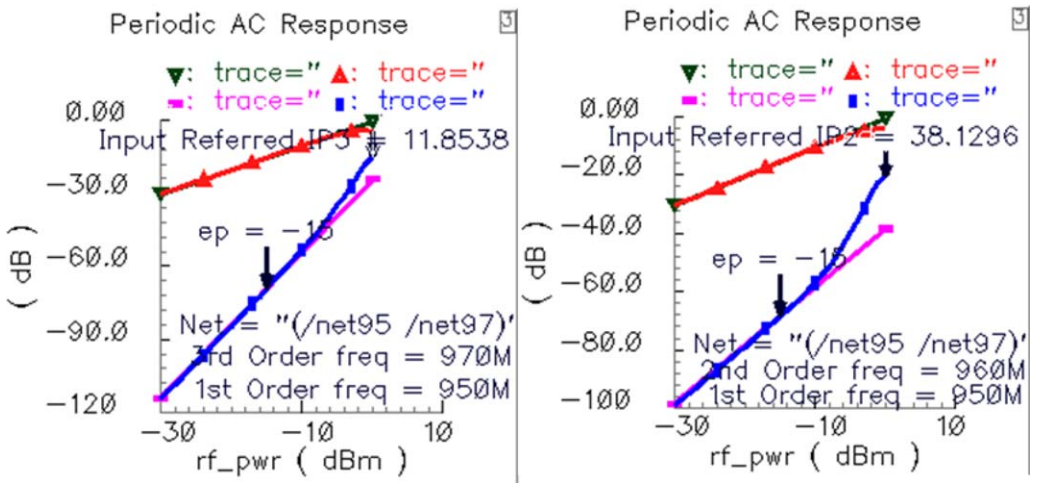

Figure 14 The measured results of IIP2 and IIP3 of the SDC. [Color figure can be viewed in the online issue, which is available at wileyonlinelibrary.com]

4. CONCLUSION

A broadband LNA/mixer is proposed, designed, and fabricated using a 0.18-μm mixed mode RF CMOS process to achieve the broadband properties for applications in DVB-S2 receiver tuner. Positive feedback is introduced to achieve the broadband characteristics in designing the LNA and an SDC is designed according to the current mirror structure for achieving the broadband characteristics and high linearity of the mixer. The good noise figure (NF) performance of LNA with high-gain mode and high linearity characteristics in low-gain mode is achieved by adding two attenuators. The total gain is controlled with 3-dB steps by the 3·6·9 dB attenuator. Moreover, a cross-coupled capacitor and a current source binding differential load are used for the low phase and amplitude mismatch properties of SDC.

ACKNOWLEDGMENTS

This research was supported by Basic Science Research Program and Nano-Material Technology Development Program through the National Research Foundation of Korea (NRF) funded by the Ministry of Science, ICT & Future Planning (No. 2011-0030079) and (No. 2009-0082580) and a grant supported from the Korean government (MEST) No. 2012R1A1A2004366 and (MSIP) No. 2014R1A1A1005901. This work was also supported by a Research Grant of Kwangwoon University in 2014.

REFERENCES

1. Y. Tsividis, Operation and modeling of the MOS transistor, McGraw-Hill, Boston, 1998.
2. V. Mignone, M.A. Vazquez-Castro, and T. Stockhammer, The future of satellite TV: The wide range of applications of the DVB-S2 standard and perspectives, Proc IEEE 99 (2011), 1905–1921.
3. M. Allegue-Martinez, N. Kelly, and A. Zhu, Digital linear precompensation technique to enhance predistortion performance in multicarrier DVB-S2 satellite communication systems, Electron Lett 50 (2014), 957–959.
4. ETSI, Digital Video Broadcasting (DVB); Second generation framing structure, channel coding and modulation systems for Broadcasting, Interactive Services, News Gathering and other broadband satellite applications (DVB-S2), EN 302 307, V1.2.1, April 2009.
5. ENSI, Digital Video Broadcasting (DVB) User guidelines for the second generation system for Broadcasting, Interactive Services, News Gathering and other broadband satellite applications (DVB-S2), TR 102 376, V1.1.1, February 2005.
6. A. Morello and V. Mignone, DVB-S2—ready for lift off, EBU Tech Rev (2004).
7. DVB Fact Sheet, 2nd Generation Terrestrial, December. 2014.
8. L.E. Larson, RF and microwave circuit design for wireless communications, Artech House Publishers, 1996.
9. K.L. Fong and R.G. Meyer, The second generation standard for satellite broad-band services, Proc IEEE 94 (2006), 210–227.
10. P. Westerguard, Recent trends in CMOS low noise amplifiers, ECE 1371 Analog Electronics II, 2011.
11. S.C. Shin, C.S. Lin, M.D. Tsai, K.Y. Lin, and H. Wang, A low-voltage and variable-gain distributes amplifier for 3.1–10.6 GHz UWB systems, IEEE Microwave Wireless Compon Lett 16 (2006), 179–181.
12. S.J. Kim, J.Y. Lee, J.C. Lee, J.H. Kim, B. Lee, and N.Y. Kim, Adaptive feedback interference cancellation system (AF-ICS), In: IEEE MTT-S International Microwave Symposium Digest, Vol. 1, Philadelphia, PA, 2003, pp. 627–630.
13. Technical brief SWRA030, Understanding and enhancing sensitivity in receivers for wireless applications, Taxas Instruments, Dallas, TX, 1999.
14. B. Razavi, RF microelectronics, The Prentice Hall, Upper Saddle River, NJ, 1998, pp. 11–25, pp. 166–200.

MICROWAVE BACKSCATTERING OF A SPHERICAL CONDUCTOR COATED BY LOSSLESS METAMATERIALS WITH AN INTERVENING AIR GAP

Adnan G. Jamil and Tenneti C. K. Rao
Department of Electrical and Computer Engineering, University of Massachusetts Lowell, 1 University Avenue, Lowell, MA 01854; Corresponding author: metamaterial.jamil@gmail.com

Received 23 February 2015

ABSTRACT: *A theoretical study of the electromagnetic backscattering from a lossless metamaterial (MTM) coated conducting sphere with an intervening air gap is presented in this article. The boundary-value technique is used to obtain the normalized backscattering cross section. A comparison of backscattering characteristics is provided using different kinds of MTMs for the coating. The MTM coating combined with the added feature of an air gap (practically realized by replacing air with styrofoam) indicate that it is possible to achieve low EM backscattering over a broad range of frequencies for certain cases.* © 2015 Wiley Periodicals, Inc. Microwave Opt Technol Lett 57:2099–2104, 2015; View this article online at wileyonlinelibrary.com. DOI 10.1002/mop.29266

Key words: *metamaterials; cloaking; scattering; radar cross section; backscattering*

1. INTRODUCTION

Electromagnetic scattering characteristic of a conducting sphere, coated (single layered or multilayered) with different kinds of materials, is a thoroughly researched and analyzed problem [1–11]. Metamaterial (MTM) coated conducting spheres came to the limelight only recently [12–16]. In [12], Wang et al. did a theoretical study, based on finite difference time-domain (FDTD) simulations, on a perfect electrical conductor (PEC) sphere coated with double negative MTMs. Cheng et al. [13] looked at Anisotropic Nihility media. Nihility media is the special kind of MTM with a refractive index of zero or near to it. Qiu et al. [14] proposed a practical realization of electromagnetic spherical cloaking by layered structure of homogenous isotropic materials. By the utilization of a discretized multilayered (>2) configuration, the authors managed to demonstrate the cloaking of a PEC sphere. In Chen et al. [15], the authors designed a cloak based on alternating thin layers of isotropic coating. In [16], Haghparast et al. studied the reduction of backscattering from a conducting sphere coated with a single layer of MTM. We propose a unique cloak design which utilizes MTMs coating the conducting sphere with an intervening air gap. The air gap may be practically realized by the use of Styrofoam which has a dielectric constant of roughly 1.03. The results in this article demonstrate the possibility of designing devices such as low-observable spherical antennas with optimized geometry and material properties or noninvasive medical sensors.

2. THEORY

Figure 1 shows the geometry of the problem. A PEC sphere of radius a, is covered by a layer of MTM in the region $b \leq \rho \leq c$ (layer-II) and, thus, an air or styrofoam gap exists between the two in the region $a \leq \rho \leq b$ (layer-I). The structure is illuminated by a circularly polarized (left or right circular) EM wave incident at an angle of 0° with respect to the z-axis. The incident wave illuminating the structure is a superposition of an electric field component (TM^r) and a magnetic field component (TE^r). In either case, the scalar magnetic and electric potential functions, A and F, respectively, are solved for from the scalar wave